PHOSPHATE TRANSPORTER TRAFFIC FACILITATOR1 Is a Plant-Specific SEC12-Related Protein That Enables the Endoplasmic Reticulum Exit of a High-Affinity Phosphate Transporter in *Arabidopsis* [W]

Esperanza González, Roberto Solano, Vicente Rubio, Antonio Leyva, and Javier Paz-Ares[1]

Centro Nacional de Biotecnología–Consejo Superior de Investigaciones Científicas, Campus de Cantoblanco, Madrid E-28049, Spain

PHOSPHATE TRANSPORTER1 (*PHT1*) genes encode phosphate (Pi) transporters that play a fundamental role in Pi acquisition and remobilization in plants. Mutation of the *Arabidopsis thaliana PHOSPHATE TRANSPORTER TRAFFIC FACILITATOR1* (*PHF1*) impairs Pi transport, resulting in the constitutive expression of many Pi starvation–induced genes, increased arsenate resistance, and reduced Pi accumulation. *PHF1* expression was detected in all tissues, particularly in roots, flowers, and senescing leaves, and was induced by Pi starvation, thus mimicking the expression patterns of the whole *PHT1* gene family. PHF1 was localized in endoplasmic reticulum (ER), and mutation of PHF1 resulted in ER retention and reduced accumulation of the plasma membrane PHT1;1 transporter. By contrast, the PIP2A plasma membrane protein was not mislocalized, and the secretion of Pi starvation–induced RNases was not affected in the mutant. *PHF1* encodes a plant-specific protein structurally related to the SEC12 proteins of the early secretory pathway. However, PHF1 lacks most of the conserved residues in SEC12 proteins essential as guanine nucleotide exchange factors. Although it functions in early secretory trafficking, PHF1 likely evolved a novel mechanism accompanying functional specialization on Pi transporters. The identification of PHF1 reveals that plants are also endowed with accessory proteins specific for selected plasma membrane proteins, allowing their exit from the ER, and that these ER exit cofactors may have a phylum-specific origin.

INTRODUCTION

Phosphorus is an essential macronutrient for all living organisms. As a constituent of nucleic acids, phospholipids, and cellular metabolites, living cells require millimolar amounts of P. Such a high demand for P poses an important problem for plants, which acquire P directly from their environment. Although P is abundant in ecosystems, phosphate (Pi), the form in which P is assimilable, is unevenly distributed in soils, and most soil Pi is immobile and not readily available to roots (Raghothama, 1999). Plants have evolved responses to adapt their growth to conditions of limited Pi supply, one of which is the activation of high-affinity Pi transport, which enhances Pi acquisition (reviewed in Raghothama, 1999; Rausch and Bucher, 2002; Ticconi and Abel, 2004).

High-affinity plant Pi transporters are proteins with 12 transmembrane-spanning domains, which were originally identified by sequence similarity to the high-affinity transporter of yeast, PHO84. Genes encoding some of these transporters can complement *pho84* yeast mutants (for review, see Rausch and Bucher, 2002). These proteins belong to the PHOSPHATE TRANSPORTER1

(PHT1) family of Pi/H$^+$ symporters (Rausch and Bucher, 2002). Nine *PHT1* genes have been identified in *Arabidopsis thaliana*, and 13 have been identified in rice (*Oryza sativa*) (Goff et al., 2002; Rausch and Bucher, 2002). Like PHO84 in yeast, members of the PHT1 family localize to the plasma membrane (Chiou et al., 2001; Shin et al., 2004).

In agreement with the central role of high-affinity Pi transporters in Pi acquisition during Pi starvation in plants, most if not all plant PHT1 transporters studied to date are expressed in roots and induced by Pi starvation (Karthikeyan et al., 2002; Mudge et al., 2002). Moreover, one member, PHT1;1 (also known as PT1), displays reduced expression in mutants of *PHOSPHATE STARVATION RESPONSE1* (*PHR1*), a gene encoding a key transcription factor regulating Pi starvation responses (Rubio et al., 2001). In addition, like other genes of the Pi starvation regulon, expression of *PHT1;1* is repressed by cytokinins and stimulated by sugars (Lejay et al., 2003; Franco-Zorrilla et al., 2005). Expression of many of these transporters is also detected in roots of plants grown under Pi-sufficient conditions and in other parts of the plant, particularly flowers and senescing leaves, suggesting that PHT1 transporters also play roles other than Pi acquisition in Pi-poor soils, such as Pi acquisition in Pi-rich soils and Pi translocation within the plant (Mudge et al., 2002). Confirming this, recent studies have shown that *pht1;1* and *pht1;4*, as well as the double mutant, show reduced Pi accumulation when grown under high-Pi regimens (Shin et al., 2004).

Another determinant of the activity of Pi transporters is the organization of their trafficking through the secretory pathway to

the plasma membrane. Numerous studies, particularly in yeast and animal cells, have shown that the first, crucial step in secretory trafficking is exit from the endoplasmic reticulum (ER) to the Golgi apparatus, which is mediated by COPII vesicles (reviewed in Barlowe, 2003). Formation of COPII is initiated by the SAR1 GTPase, which, upon activation by SEC12, a guanine nucleotide exchange factor, promotes the recruitment of COPII vesicle coats and cargo selection (Barlowe and Schekman, 1993; Barlowe, 2003). Cargo incorporation in COPII requires the establishment and maintenance of the secretion-competent conformation of cargo proteins, which often requires the assistance of cargo-specific accessory proteins (reviewed in Herrmann et al., 1999; Barlowe, 2003). Additionally, some cargo proteins are not recognized by general components of COPII and need the assistance of specific transport receptors to be included in COPII (Herrmann et al., 1999; Barlowe, 2003). One example of such an accessory protein is PHO86 of yeast, which is required for the ER exit of the PHO84 transporter. Like *PHO84*, *PHO86* is regulated by the Pi starvation (PHO) signaling pathway (Lau et al., 2000). In plants, the requirement for such accessory proteins has not yet been demonstrated for Pi transporters or other proteins entering the secretory pathway. In fact, some reports suggest a bulk-flow model for ER exit, at least for soluble proteins (Crofts et al., 1999; Phillipson et al., 2001). No *PHO86*-related genes have been detected in the *Arabidopsis* genome, despite the sequence similarities between PHO84 from yeast and the high-affinity Pi transporters from plants and the presence of SEC12, SAR1, and other general components of the COPII coat in plants (for reviews, see Neumann et al., 2003; Sanderfoot and Raikhel, 2003; Jurgens, 2004).

In this study, we report the isolation and characterization of the *PHOSPHATE TRANSPORTER TRAFFIC FACILITATOR1* (*PHF1*) gene, mutation of which gives phenotypes characteristic of a specific impairment in Pi uptake. We show that PHF1 has the functional characteristics of accessory proteins of the secretory pathway, like PHO86 from yeast, displaying specificity toward selected cargo proteins (Pi transporters in this case), and thus provides evidence that plants are also endowed with accessory proteins. PHF1 is a plant-specific SEC12-related protein, which is structurally unrelated to PHO86, indicating that accessory proteins may have evolved independently in organisms from different phyla even though they are involved in the trafficking of structurally and functionally related transporter proteins.

RESULTS

Isolation of a Pi Starvation Response Mutant

We screened an ethyl methanesulfonate–mutagenized M2 population of a transgenic line harboring the Pi starvation–responsive *IPS1*:β-*glucuronidase* (*GUS*) reporter gene (Rubio et al., 2001) for mutants displaying constitutive expression of *IPS1:GUS*, as assessed using a nondestructive GUS staining assay (Martin et al., 2000; Rubio et al., 2001). Putative mutants were identified as follows. Nine-day-old seedlings (~20,000) grown in Pi-rich medium were stained for GUS activity for 5 h, during which time plates were examined every hour. Two seedlings showing GUS

activity were selected, and M3 progeny were obtained for both of them. After preliminary phenotypic analysis, one of the mutants, constitutively displaying many Pi starvation responses and high arsenate resistance (see below), was selected for further analysis. The corresponding gene was named *PHF1* after functional characterization (see below).

We took advantage of the increased arsenate resistance phenotype of *phf1-1* to screen for additional *phf1* alleles. After prescreening 50,000 seedlings for arsenate resistance (large roots with hairs in plants grown in 10 ppm arsenate), followed by analysis of GUS activity in the progeny, we identified a single additional mutant (*phf1-2*) resembling *phf1-1* phenotypically. Results from crossing experiments indicated that the mutants were recessive and allelic (data not shown). For further analysis, the *phf1-1* allele was backcrossed three times with the wild-type transgenic reporter line.

phf1 Displays Phenotypes Associated with Impaired Pi Uptake

Several developmental and metabolic traits influenced by Pi starvation and the expression of five Pi starvation response genes were analyzed. For the analysis of developmental and metabolic traits, plants were grown under different Pi regimens. The *phf1* mutation resulted in visible *IPS1:GUS* activity in plants grown under a Pi-rich regimen, although when grown in a Pi-deficient medium, GUS activity was lower in *phf1* than in wild-type plants (Figure 1A). In addition, both *phf1* alleles displayed reduced growth under low-Pi regimens, increased anthocyanin accumulation (evident in plants grown at moderately low Pi concentrations), and increased root hair number and size, compared with wild-type plants, as shown in Figure 1B for *phf1-1*. This effect of the mutations on growth and anthocyanin accumulation was not general for other nutrients, as mutants and wild-type plants were indistinguishable when grown under different nitrogen regimens (data not shown). *phf1* mutant alleles also displayed an increased root-to-shoot growth ratio when grown under Pi-rich conditions (P < 0.02, using Student's *t* test), but as with GUS activity, the root-to-shoot growth ratio was reduced in both alleles compared with wild-type plants when assayed in Pi-starved plants (although only for the *phf1-2* allele was the difference statistically significant; P < 0.03) (Figure 1C). The analysis of Pi content revealed that mutation of *PHF1* impairs Pi accumulation when grown under high-Pi conditions (Figure 1C). To evaluate whether the effect on Pi accumulation could be attributable to impaired Pi uptake, we performed Pi uptake experiments and as a control we also examined SO_4^{2-} uptake (Figure 1C). Wild-type plants grown in low Pi (60 μM) could take up five times more Pi than the *phf1* mutant (P < 0.006), whereas no statistically significant difference between the wild type and mutant was observed when SO_4^{2-} uptake was analyzed under similar conditions.

To confirm that Pi uptake was affected in the *phf1* mutants, we measured arsenate resistance. Arsenate is an ion structurally analogous to Pi and is transported into plants through the high-affinity Pi transporters (Asher and Reay, 1979; Shin et al., 2004). *phf1* mutants displayed higher arsenate resistance than wild-type plants, particularly in a larger development of the root
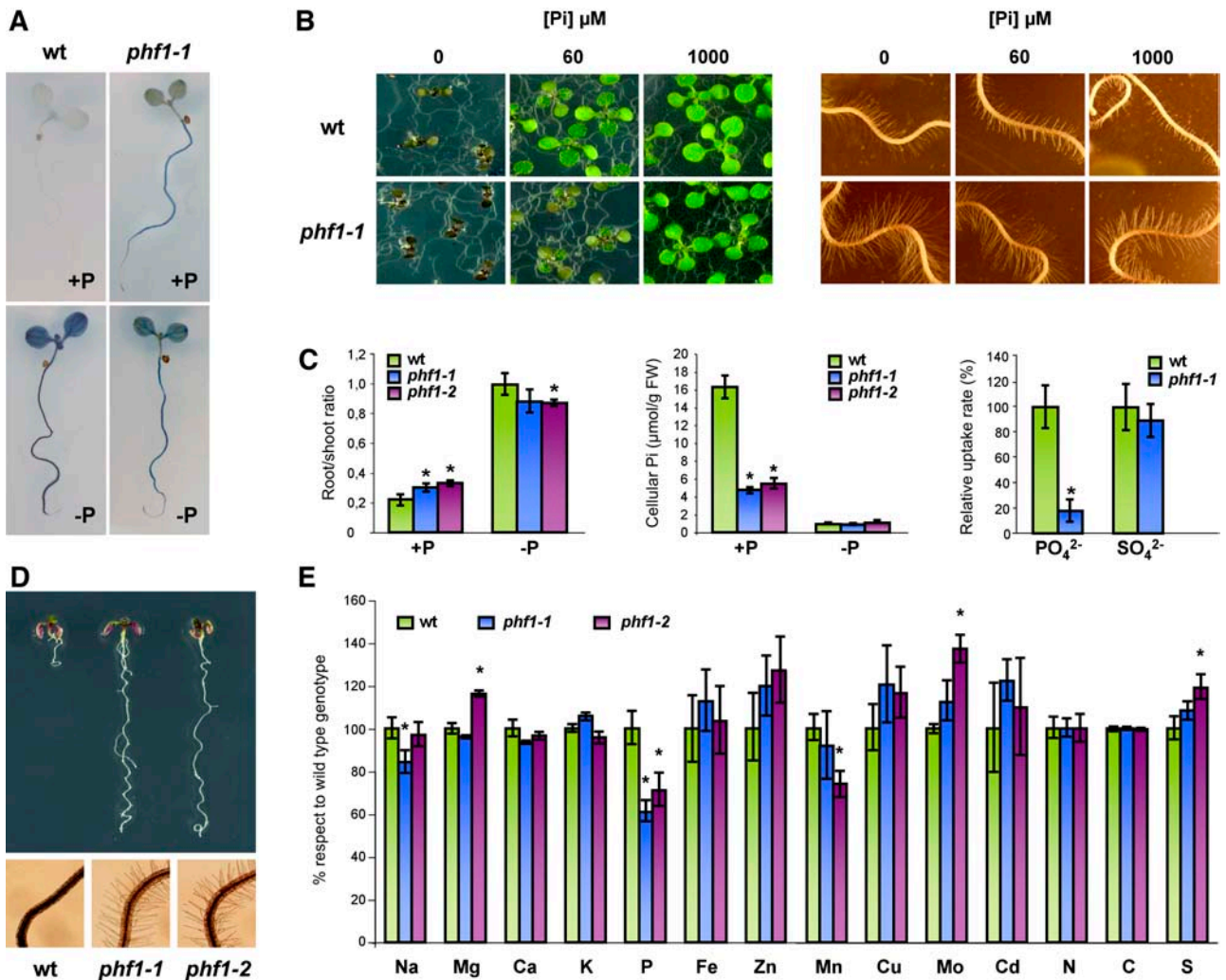
Figure 1. Phenotypic Characteristics Associated with the *phf1* Mutant Alleles.

(A) Histochemical analysis of GUS activity driven by the *IPS1:GUS* reporter gene in wild-type and *phf1-1* plants grown in Pi-rich (+P) or Pi-deficient (−P) medium.

(B) Wild-type and *phf1-1* plants after growth on medium containing 0, 60, or 1000 µM Pi (left). Details of their root hairs are shown at right.

(C) Histograms of root/shoot growth ratio, cellular Pi content, and Pi and SO_4^{2-} uptake for the wild type and *phf1* mutants. FW, fresh weight.

(D) Wild-type, *phf1-1*, and *phf1-2* plants after growth in Pi-deficient medium supplemented with 10 ppm arsenate.

(E) Histogram showing the relative contents of different elements in the wild type and *phf1* mutant alleles after growth in complete medium.

In all instances, plants were grown for 12 d, except for the histochemical staining **(A)**, root hair growth **(B)**, and Pi and SO_4^{2-} uptake **(C)** experiments, in which plants were grown for 5, 5, and 8 d, respectively. Standard deviations are indicated by error bars. Statistically significant differences between the wild type and either allele (P < 0.05, according to Student's *t* test) are marked with asterisks.

system, including root hairs, compared with that of the wild type when grown in the presence of this toxic compound (Figure 1D).

To evaluate the degree of specificity of the *phf1* mutation on Pi uptake, we performed elemental analysis of mutant and wild-type plants grown in complete medium (Figure 1E). The greatest difference between the wild type and mutants was in P content, which was reduced to 60% of wild-type levels in the mutants (P < 0.02). Additionally, the content of other elements was different in the wild type and mutants, although these differences were not statistically significant for either of the two alleles and in most

cases were the result of increased rather than decreased accumulation of these elements.

The effect of the *phf1* mutant alleles on the expression of Pi starvation–responsive genes was examined using RNA gel blot analysis. Five *Arabidopsis* Pi starvation–responsive genes were analyzed: *IPS1* and *At4*, members of the *MT4/TPS1* family, and *PHT1;1*, *ATACP5*, and *RNS1*, encoding a high-affinity Pi transporter, an acid phosphatase, and a RNase, respectively (reviewed in Franco-Zorrilla et al., 2004). For all genes except *RNS1*, expression was enhanced in the mutants compared with the wild

type during growth under Pi-rich conditions (Figure 2A). In plants grown in Pi-deficient medium, gene expression was further increased both in the wild type and in mutant plants. However, in this case, Pi starvation–responsive genes displayed reduced expression in the mutant compared with the wild type, with the exception of *RNS1*, whose expression was unaltered by the *phf1* mutations (Figure 2A).

The reason for this effect on the expression of Pi starvation–responsive genes in the mutant grown under Pi-limiting conditions needs to be investigated further, but we have observed that a mutation of the Pi transporter, PHT1;1, also results in reductions in many Pi starvation responses (P. Catarecha, M.D.

Figure 2. Effect of *phf1* Mutations on the Expression of Pi Starvation–Responsive Genes.

(A) RNA gel blot analysis of the expression of Pi-responsive genes. RNA was prepared from roots (R) and shoots (S) of the wild type and *phf1-1* and *phf1-2* mutants grown for 8 d in Pi-rich or Pi-deficient medium. RNA gel blots containing 15 μg of RNA were successively hybridized to the probes corresponding to the Pi starvation–responsive genes indicated. Hybridization to a probe corresponding to 18S RNA was used as a loading control. **(B)** Histochemical analysis of GUS activity driven by the *IPS1*:*GUS* reporter gene. Plants were grown in Pi-deficient medium with or without kinetin (left) or in low-Pi (50 μM) medium with sucrose (1 or 3%, right) or without sucrose (0%).

Segura, B.G. de León, R. Solano, L. Romero, J. Paz-Ares, and A. Leyva, unpublished data).

Pi starvation–responsive genes are affected by cytokinins and sugars, which repress and stimulate their expression, respectively (Franco-Zorrilla et al., 2005). To determine whether the effects of these signaling molecules are altered in *phf1* mutants, we examined the effects of the mutations on *IPS1*:*GUS* activity upon treatment with sugars and cytokinins (Figure 2B). The response of *phf1* mutants to cytokinins and sucrose was similar to that of wild-type plants.

Together, these data indicate that *phf1* affects Pi transport directly and that this effect is largely specific to this nutrient, because transport of other nutrients/signaling molecules is greatly unaffected in *phf1* mutants.

PHF1 Encodes a SEC12-Related Plant-Specific Protein

To understand how PHF1 works, we first undertook positional cloning on the basis of a cross between the *phf1-1* mutant allele (Columbia [Col-0] ecotype) and the Landsberg *erecta* (L*er*) background. Genotyping of 500 mutant plants allowed us to map the mutation on chromosome 3 to a region of ~150 kb between genes At3g51895 and At3g52360 (Figure 3A). Two candidate genes were selected in this region on the basis of Pi starvation responsiveness (At3g52180 and At3g52190; our unpublished results based on microarray transcriptome-wide analysis of the effect of Pi starvation on gene expression). Sequencing of the At3g52190 gene, whose Pi starvation responsiveness was also detected by Misson et al. (2005) in microarray-based experiments, revealed that it contained mutations in both *phf1* alleles (G-to-A transitions in nucleotides 81 and 960 of the coding sequence, respectively, in which the A of the predicted start codon is defined as nucleotide 1), which results in the replacement of Trp residues (Trp-27 and Trp-320, respectively) with stop codons (Figure 3A).

Transformation of the *phf1-1* allele with a genomic region of 6 kb, spanning the coding region of At3g52190 plus sequences 2.7 kb upstream of the start codon and 0.5 kb downstream of the stop codon, or with a cDNA spanning the whole coding region (see Methods) under the control of the 35S promoter of *Cauliflower mosaic virus*, rescued the wild-type phenotype in 9 of 13 and 10 of 15 transformants, respectively, as shown in Figure 3B with respect to *IPS1*:*GUS* expression and arsenate resistance.

The *PHF1* mRNA translates into a hypothetical protein of 398 amino acid residues. Database searches identified highly related proteins in various plants (tomato [*Lycopersicon esculentum*] and rice, the latter shown in Figure 3C), representing putative functional homologs. Significant similarities were also found with members of the SEC12 family, especially from plants (Figure 3C). The SEC12 family consists of a group of proteins quite heterogeneous in primary structure, participating in the formation of COPII vesicles involved in the ER exit of proteins entering the secretory system. Despite sequence divergence, all SEC12 proteins are type II integral membrane proteins located in the ER, with a cytoplasmic domain displaying guanine exchange factor activity predicted to adopt a β-propeller structure with seven WD40 repeats (Chardin and Callebaut, 2002).

Sequence alignment of PHF1 with putative homologs from rice and tomato, and members of the SEC12 protein family from
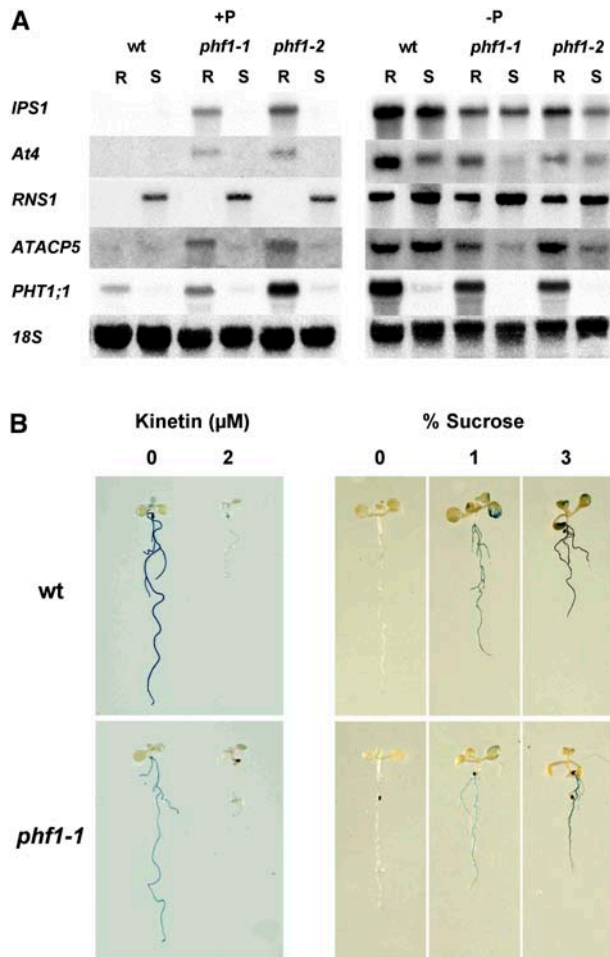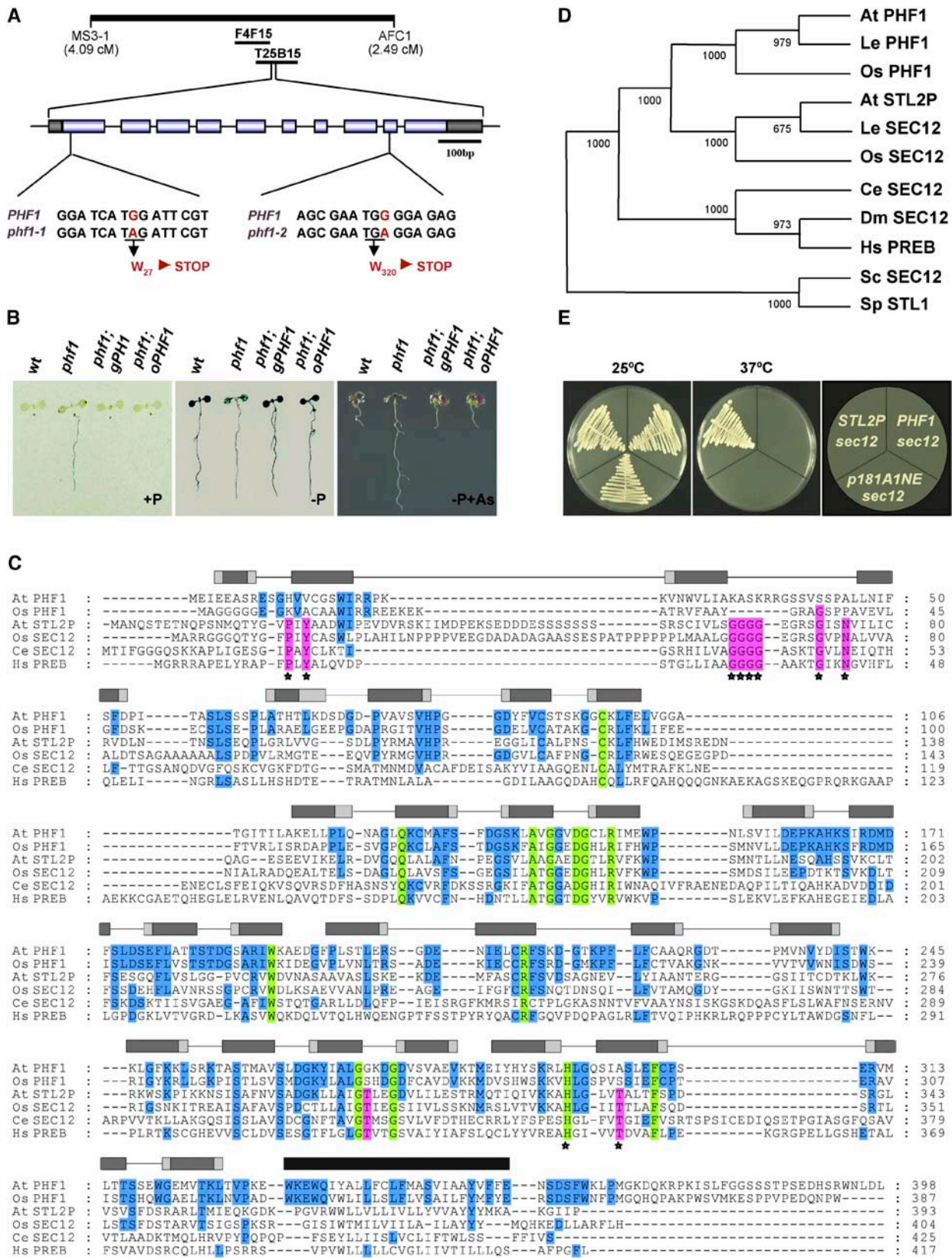
Figure 3. Positional Cloning of PHF1 and the Characteristics of Its Protein.

plants, animals, and fungi (Figure 3C; only a subset of known SEC12/PHF1 sequences is shown, but residues conserved among all known SEC12 proteins are highlighted), revealed that out of the 156 residues conserved within PHF1 homologs, 50 were conserved in all plant SEC12 proteins analyzed. Additionally, out of the 23 residues conserved between plant and animal SEC12 proteins, 13 are conserved in all PHF1 homologs, more than that conserved between all SEC12 proteins (10 residues). Notably, however, out of the 10 residues shared by all known SEC12 proteins, only 1 is conserved in the PHF1 proteins examined, strongly suggesting functional specialization of PHF1 involving a mechanism of action divergent from that of SEC12 (see Discussion).

Overall structural conservation was first evaluated using the structure prediction metaserver GENESILICO (Kurowski and Bujnicki, 2003), which predicted that PHF1 proteins have seven WD40 repeats related to the C-terminal region of Tup1 (score 1^{e-81}; Sprague et al., 2000). These seven WD40 repeats are very similar to those predicted by Chardin and Callebaut (2002) for SEC12 proteins, suggesting strongly that, despite functional divergence, overall secondary structure is conserved between PHF1 and SEC12 proteins. Additionally, the use of the SMART program (Letunic et al., 2004) predicted a transmembrane domain in all PHF1 and SEC12 proteins. A premature stop codon in both *phf1-1* and *phf1-2* eliminates this transmembrane domain in the encoded proteins and probably results in complete loss of function.

A phylogram of representative PHF1 and SEC12 proteins was constructed using PHYLIP software (Felsenstein, 1989) (Figure 3D; Supplemental Figure 1 online shows the alignment of all SEC12/PHF1 sequences used to construct the phylogram). The result showed a close phylogenetic relation between PHF1 and plant SEC12 proteins (bootstrap value for the node separating proteins from the plant phyla: 1000 out of 1000 samples; Figure 3D), indicating that most likely PHF1 proteins originated from a plant-specific SEC12 ancestral protein.

In conclusion, PHF1 displays remarkable structural similarity to SEC12 proteins but lacks highly conserved residues in SEC12 proteins. To gain insights into the functional implications of these differences between PHF1 and SEC12, we examined whether *Arabidopsis* PHF1 could functionally replace SEC12 in yeast. To this end, we cloned *Arabidopsis PHF1* and *SEC12* (*STL2P*) open reading frames in p181A1NE (Leggewie et al., 1997) under the control of the constitutive ADH promoter and transformed a temperature-sensitive *sec12* mutant of yeast. In accordance with previous reports (d'Enfert et al., 1992), *Arabidopsis* SEC12 (STL2P) could rescue the growth defect of the mutant yeast at 37°C; however, PHF1 could not (Figure 3E).

ER Localization of a Functional PHF1:GFP Protein

To gain information on the cellular function of PHF1, we examined its subcellular localization. Two chimeric genes were prepared, one corresponding to a fusion between the promoter plus the coding region of *PHF1* and the green fluorescent protein (*GFP*) coding region at the 3′ end. In the second, the promoter region of *PHF1* was replaced by the 35S promoter. In both cases, the fusion protein could rescue the wild-type phenotype of *phf1*, indicating functionality of the reporter protein (see Supplemental Figure 2 online). Confocal microscopy was used to examine the subcellular localization of the fusion proteins in Pi-starved plants. The PHF1:GFP protein expressed from both constructs emitted a fluorescence signal (Figure 4) resembling that of ER-localized proteins. In epidermis of *35S:PHF1:GFP* plants, fluorescence of the reticulate network and of typical patches where ER lamellae converge was very evident (Figure 4B). To further assess the ER localization of PHF1, a transgenic plant harboring *35S:PHF1:GFP* was bombarded with an ER marker prepared according to Haseloff et al. (1997). The marker consisted of the coding region of *DsRed2* fused at its 5′ end to a sequence encoding a signal peptide and at its 3′ end to an oligonucleotide encoding an ER retention signal (KDEL; see Methods). As shown

---

Figure 3. (continued).

(A) Scheme of the position of PHF1 on chromosome 3 of *Arabidopsis*, between markers MS3-1 and AFC1. The exon structure of PHF1 is represented with boxes (dark, untranslated; light, coding region). The sequence surrounding the mutations (G-to-A transitions) in *phf1-1* and *phf1-2* is also shown.
(B) Complementation of *phf1*. Histochemical analysis of IPS1:GUS activity in plants grown in Pi-rich (left) or Pi-deficient (middle) medium, and phenotype of plants grown in the presence of 10 ppm arsenate (right). The genetic constitution of the plants is as follows: wild type; *phf1-1* (*phf1*); and *phf1-1* transformed with a 6-kb genomic region corresponding to the *PHF1* gene (*phf1; gPHF1*) or with the coding region under the control of the promoter of the 35S gene of *Cauliflower mosaic virus* (*phf1; oPHF1*).
(C) Alignment of *Arabidopsis* PHF1 with presumed functional PHF1 homologs and with SEC12 proteins using the program T-COFFEE (Notredame et al., 2000), structural predictions using the GENESILICO metaserver (Kurowski and Bujnicki, 2003), and the SMART program (Letunic et al., 2004). The seven predicted WD repeats are indicated by gray boxes representing the predicted β-strands within each single WD (arranged in a D-to-C configuration). The dark areas in each box represent core regions predicted by the two secondary prediction methods in GENESILICO; light areas represent regions predicted by only one of the methods. The predicted transmembrane domain is indicated by a black rectangle. Colored in green are amino acid residues conserved in all PHF1 and SEC12 proteins from plants or animals used in **(D)**; only a subset of the sequences are shown. Blue indicates amino acid residues conserved in all PHF1 proteins; pink indicates amino acid residues conserved in all plant and animal SEC12 proteins. Asterisks highlight amino acid residues conserved in all SEC12 proteins.
(D) Phylogram of PHF1 and SEC12 proteins constructed with the PHYLIP software (Felsenstein, 1989). The bootstrapping value (out of 1000 samples) for each node, obtained with the same software, is shown. The proteins are as follows: AtPHF1 (*Arabidopsis* PHF1); LePHF1 (*Lycopersicon esculentum*); OsPHF1 (*Oryza sativa*); AtSTL2P (*Arabidopsis* SEC12 ortholog); OsSEC12 (*O. sativa*); CeSEC12 (*Caenorhabditis elegans*); DmSEC12 (*Drosophila melanogaster*); HsPREB (*Homo sapiens*); ScSEC12 (*Saccharomyces cerevisiae*); SpSTL1 (*Schizosaccharomyces pombe*).
(E) Complementation tests with the temperature-sensitive *sec12* mutant from *S. cerevisiae sec12* mutant cells transformed with empty vector (p181A1NE) or with vector expressing the STL2P open reading frame or PHF1 open reading frame grown at 25 and 37°C for 3 d.
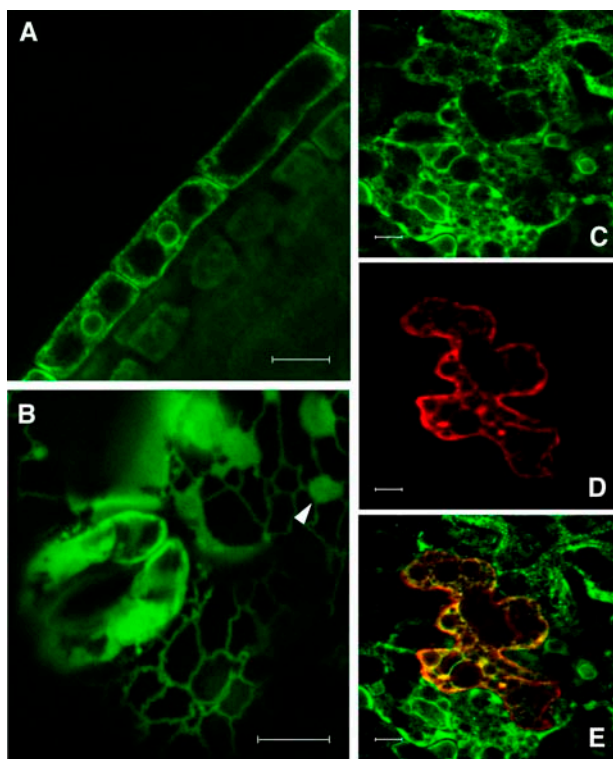
Figure 4. Subcellular Localization of a Functional PHF1:GFP Fusion Protein.

(A) Confocal laser scanning micrographs of Pi-starved root cells expressing *PHF1:GFP* from the *PHF1* promoter.

(B) Micrographs of Pi-starved leaf epidermal cells from a transgenic line harboring the *35S:PHF1:GFP* construct, in which fluorescence highlights a polygonal network of ER tubules interspersed with small patches of ER lamellae, one of which is indicated with a white arrowhead.

(C) to **(E)** Micrographs of Pi-starved leaf epidermal cells from a transgenic line harboring the *35S:PHF1:GFP* construct bombarded with a construct encoding an ER-located marker (*35S:DsRed2:KDEL*). The images shown correspond to PHF1:GFP **(C)**, DsRed2:KDEL **(D)**, or an overlay of the two **(E)**.

Bars = 10 μm.

in Figure 4, both fluorescence signals greatly overlap, establishing the localization of PHF1. The ER localization of PHF1 was also inferred with high confidence using LOPIT (for Localization of Organelle Proteins by Isotope Tagging; score 0.89) (Dunkley et al., 2004; T. Dunkley and K. Lilley, personal communication).

phf1 Is Impaired in the Localization of the High-Affinity Pi Transporter PHT1;1 to the Plasma Membrane

In wild-type plants, PHT1;1 is localized to the plasma membrane, where it actively transports Pi to the cell (Chiou et al., 2001). Because *phf1* displays impaired Pi transport, we tested whether PHF1 is involved in proper trafficking of the Pi transporter to the plasma membrane. Two types of construct were prepared in which the expression of *PHT1;1:GFP* was driven by its own promoter or by the 35S promoter. These constructs were used to transform both wild-type and *phf1* plants.

Confocal microscopy revealed that in transgenic plants starved of Pi for 8 d harboring either construct, fluorescence highlighted the plasma membrane in wild-type plants (Figures 5A and 5C). In particular, in the *35S:PHT1;1:GFP* plants, the fluorescence highlighted cell junctions very clearly (Figure 5C). In contrast with wild-type plants, in *phf1* plants fluorescence by PHT1;1:GFP was observed in the ER (Figures 5B and 5D).

Localization of PHT1;1:GFP could only be studied in Pi-starved plants because of the low expression of the construct in Pi-rich plants, but it could be observed under both Pi regimens in *35S:PHT1;1:GFP* transgenic plants. In Pi-rich plants, localization of PHT1;1:GFP was also found in the plasma membrane, although cell junctions were not so evident (see Supplemental Figure 3 online), similar to the results of Chiou et al. (2001). The reason for the difference regarding the frequency/amount of PHT1;1:GFP in cell junctions between Pi-starved and nonstarved leaf epidermal cells remains to be studied.

phf1 Does Not Display Impaired General Protein Trafficking in the Endomembrane System

Several lines of circumstantial evidence, including the similar elemental compositions (excepting P) of *phf1* and wild-type
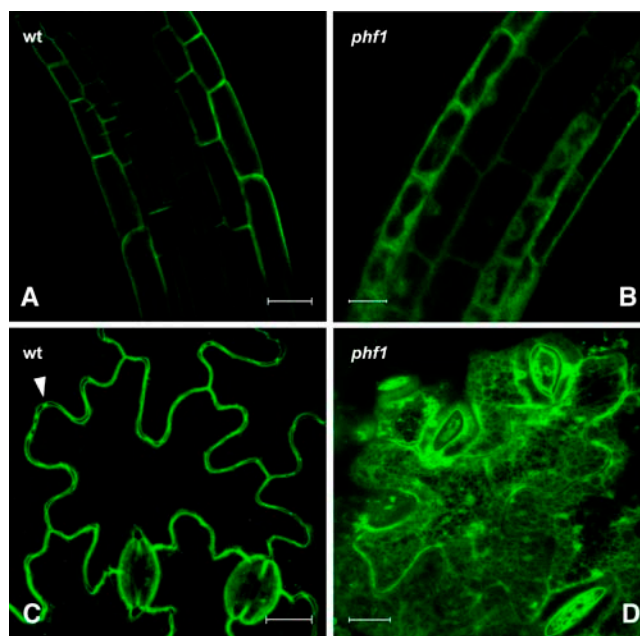

Figure 5. Subcellular Localization of PHT1;1:GFP in Wild-Type and *phf1* Plants.

(A) and **(B)** Confocal laser scanning micrographs of Pi-starved transgenic wild-type **(A)** and *phf1-1* **(B)** root cells expressing *PHT1;1:GFP* from the *PHT1;1* promoter showing fluorescence associated with the plasma membrane and the ER, respectively.

(C) and **(D)** Micrographs of leaf epidermal cells from transgenic wild-type **(C)** and *phf1-1* lines **(D)** harboring the *35S:PHT1;1:GFP* construct. In **(C)**, fluorescence highlights the plasma membrane, and a cell junction is indicated with a white arrowhead. By contrast, in **(D)**, a reticulate structure is very evident.

Bars = 10 μm.

plants and similar responses to cytokinins and sugars during the Pi starvation response, suggested that *phf1* plants did not have a general defect in protein trafficking. To confirm this, we examined the effect of the mutation on the localization of PIP2A, a plasma membrane protein unrelated to Pi nutrition, and in the secretion of Pi starvation RNases. A construct expressing the *35S:PIP2A:GFP* fusion protein (Cutler et al., 2000) was used to transform both wild-type and *phf1* plants. Confocal microscopy analysis of plants grown in rich medium revealed no differences in the subcellular localization of PIP2A between wild-type and *phf1* plants (Figure 6A).

Secreted RNase activity was analyzed both in the Pi-starved wild type and in *phf1* mutants. As with PIP2A, no difference could be detected between wild-type and mutant plants in the activity of secreted RNases (Figure 6B).

Decreased Accumulation of PHT1;1 in *phf1*

The functional characteristics of PHF1 classify this protein as an accessory protein involved in the ER exit of PHT1;1 (and probably other related Pi transporters; see Discussion). The fact that PHF1 is detected only in the ER suggests that it likely exerts its role as an outfitter (Herrmann et al., 1999), helping PHT1;1 (and possibly related proteins) to adopt a secretion-competent conformation. In agreement with this, preliminary data from the analysis of independent transgenic lines of wild-type and *phf1* plants transformed with the *35S:PHT1;1:GFP* gene construct indicated that average fluorescence was higher in the wild type than in the mutant background. To confirm this possibility on the effect of *phf1* on PHT1;1 accumulation, a wild-type transgenic line harboring a *35S:PHT1;1:GFP* gene construct at a single locus and displaying detectable levels of PHT1;1:GFP was crossed with the *phf1* mutant and with a line overexpressing PHF1, and homozygous plants were obtained for all genotypes. In these lines, PHT1;1:GFP accumulation was examined by inmunoblotting. As shown in Figure 7 (top panel), PHT1;1:GFP accumulation was lower in the mutant and higher in the PHF1 overexpressor

line than in the wild type. Moreover, RNA gel blot analysis indicated that *PHT1;1:GFP* RNA, whose expression is driven by the constitutive 35S promoter, accumulated more strongly in the *phf1* mutant than in the wild-type and PHF1-overexpressing transgenic plants (Figure 7, bottom panel). These results suggest a role for PHF1 in facilitating PHT1;1 to adopt a proper conformation and also that there is a promoter-independent feedback mechanism controlling PHT1;1 protein accumulation. Such a regulatory mechanism is also influenced by the plant Pi status, in agreement with the increased needs of Pi transport under these conditions.

Expression of *PHF1* and Control by PHR1

The study of *PHF1* expression and its possible control by the key Pi starvation transcription factor regulator PHR1 was performed using RNA gel blot analysis. First, RNA was prepared from different aerial parts of adult plants grown in soil under Pi-sufficient conditions for 4 weeks and from roots of 2-week-old plants grown on agar plates (Figure 8A). *PHF1* showed detectable expression in all organs examined and was most pronounced in flowers, senescing leaves, and roots. Subsequently, the response to different nutrient deficiencies was examined. *PHF1* again showed a basal level of expression in all types of nutrient-deficient medium, except in Pi-deficient medium, in which *PHF1* accumulation was highly enhanced. This behavior was similar to that of the Pi starvation–specific *IPS1* gene (Figure 8B) (Martin et al., 2000).

We next tested the effect of the *phr1* and *phf1* mutations on *PHF1* expression in plants grown in Pi-rich or Pi-lacking medium (Figure 8C). *PHF1* showed decreased expression in both *phr1* and *phf1* mutants compared with the wild type, although to different extents with respect to *IPS1*. The higher reduction of *phf1* mRNA in *phf1* could, in part, reflect instability of the *phf1* transcript caused by the fact that it encodes a truncated protein, and the lower reduction of *PHF1* RNA in *phr1* could reflect partial redundancy between PHR1 and related homologs, which is
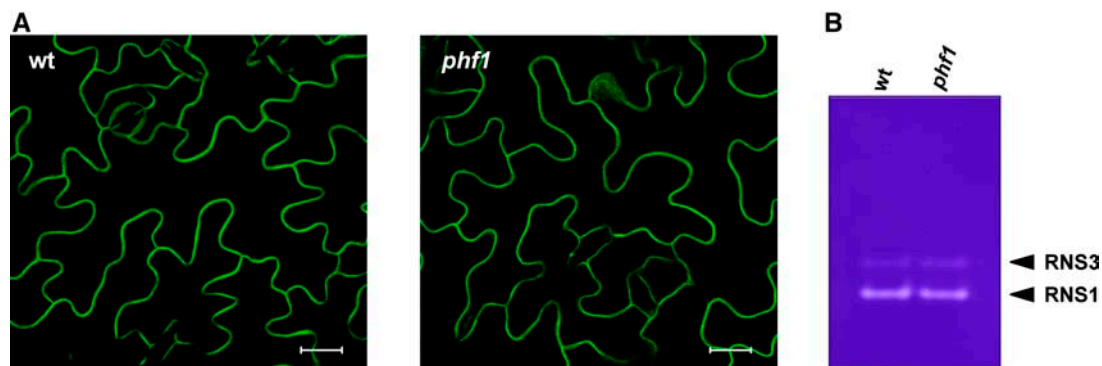

Figure 6. Subcellular Localization of PIP2A Plasma Membrane Protein and RNase Secretion in the *phf1* Mutant.

(A) Confocal micrographs of leaf epidermal cells from transgenic wild-type and *phf1-1* lines harboring the *35S:PIP2A:GFP* construct showing identical fluorescence emission, associated with the plasma membrane, in both genetic backgrounds. Bars = 20 μm.
(B) Secreted RNase activity from Pi-starved wild-type and mutant plants. Plants were grown for 5 d in complete liquid medium and then transferred for an additional 7 d to Pi-deficient medium. Secreted proteins were separated by native-PAGE electrophoresis and stained for RNase activity. The positions of secreted RNase1 and RNase3 are shown.
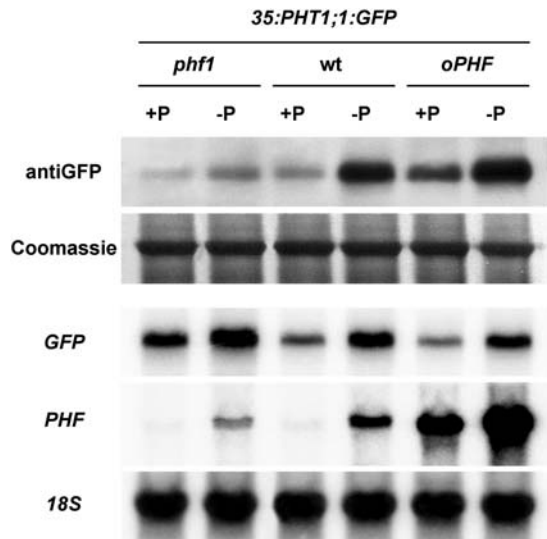
Figure 7. Analysis of the Expression of *PHT1;1:GFP* in the Wild Type, the *phf1* Mutant, and a PHF1-Overexpressing Transgenic Line.

A transgenic line having *35S:PHT1;1:GFP* at a single locus was crossed with *phf1-1* and a PHF1-overexpressing transgenic line (35S:PHF1 [oPHF1]), and homozygous *phf1*, wild-type, and 35S:PHF1 lines containing the *35S:PHT1;1:GFP* were obtained. Top, protein gel blot analysis of PHT1;1:GFP accumulation. Total protein was extracted from Pi-rich and Pi-starved plants and separated by SDS-PAGE. PHT1;1:GFP was detected by immunoblotting with anti-GFP antibody. This panel also shows Coomassie staining of the large subunit of ribulose-1,5-bis-phosphate carboxylase/oxygenase as a loading control. Bottom, RNA gel blot analysis of *PHT1;1:GFP* (*GFP*) RNA and *PHF1* RNA accumulation in the Pi-starved and nonstarved plants of different genetic constitutions. RNA gel blots containing 15 μg of RNA per track were successively hybridized to the probes indicated.

manifested differently in different Pi-responsive genes (Rubio et al., 2001).

DISCUSSION

Recent studies have revealed the importance of transcriptional control in the establishment of the responses to Pi starvation in plants (Franco-Zorrilla et al., 2004), in agreement with examples from yeast and bacteria. In this study, we discovered another important component, PHF1, necessary for the proper functioning of a key element of the Pi starvation system, the high-affinity Pi transporter. The identification of PHF1 further underlines the operational similarities between the Pi rescue system in yeast and plants and, by extension, similarities in secretory trafficking of plasma membrane proteins. However, like transcriptional control, which in plants involves the participation of a plant-specific transcription factor, PHR1, operational similarities in Pi transporter traffic between yeast and plants are not manifested through structural similarities between the specific molecular determinants of this traffic, because PHF1 is a plant-specific protein and PHO86 is yeast-specific.

PHF1 was identified in a genetic screen aimed at identifying mutants showing constitutive expression of Pi starvation re-

sponses. We anticipated identifying repressors of Pi starvation responses or, alternatively, genes affecting Pi uptake with this screen, because they would display a genetically driven Pi starvation phenotype attributable to insufficient internal accumulation of Pi, despite growth in Pi-rich medium. Indeed, these features applied to the *phf1* mutants, which displayed both reduced Pi content and Pi uptake (Figure 1). Additional phenotypic characteristics of *phf1*, such as enhanced arsenate resistance and partially activated Pi starvation responses, can be perfectly explained as a consequence of the impairment in Pi transport in the mutant.
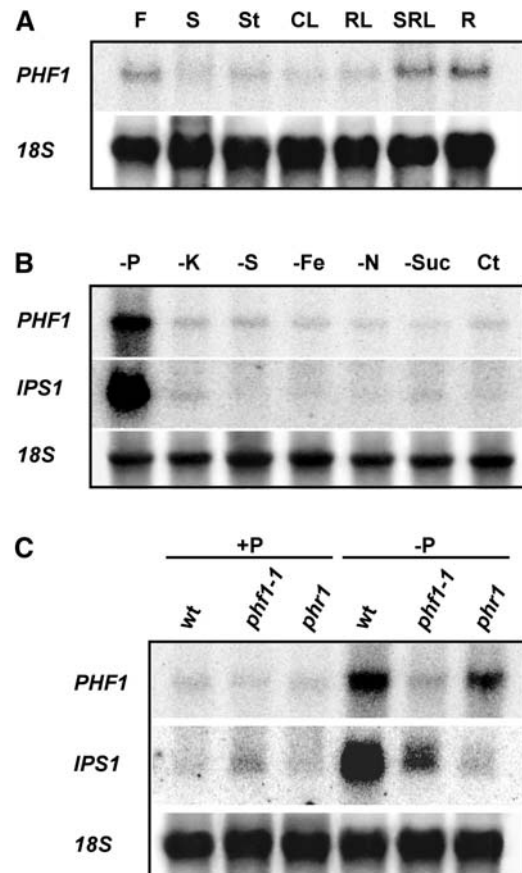

Figure 8. RNA Gel Blot Analysis of *PHF1* Responsiveness to Different Developmental and Nutritional Signals, and the Effect of *phr1*.

(A) *PHF1* expression in response to developmental cues. Wild-type plants were grown for 4 weeks in soil or 2 weeks in complete medium for root isolation, and then organs were collected independently before RNA extraction: flowers (F), siliques (S), stems (St), cauline leaves (CL), nonsenescent rosette leaves (RL), senescent rosette leaves (SRL), and roots (R).
(B) *PHF1* responsivenes to nutritional signals. RNA was extracted from total wild-type plants grown in solid medium for 5 d and then transferred for 5 d to medium containing (control [Ct]) or lacking Pi (−P), potassium (−K), sulfur (−S), iron (−Fe), nitrogen (−N), or sucrose (−Suc).
(C) *PHR1* control of *PHF1*. RNA was extracted from wild-type, *phf1-1*, and *phr1-1* plants grown for 8 d in complete (+P) or Pi-deficient (−P) medium. In all cases, RNA gel blots containing 15 μg of RNA per track were successively hybridized to the probes indicated.

Cloning and characterization of *PHF1*, and subcellular localization studies with PHF1 and the Pi transporter PHT1;1, provided insights into the molecular details of PHF1 action, which involves early secretory trafficking of Pi transporters (at least of PHT1;1). This function perfectly explains the Pi uptake defect of *phf1*. Thus, although in the wild type PHT1;1 is localized in the plasma membrane, in *phf1* PHT1;1 is retained in the ER. PHF1 has structural homology with SEC12 proteins, which are involved in general early secretory trafficking (Chardin and Callebaut, 2002). However, PHF1 proteins show striking differences from SEC12 proteins, which most likely form the basis for the specialized function of PHF1.

Several lines of evidence suggest that PHF1 plays an important and specific role in the localization of Pi transporter(s). First, PHF1 is unable to replace yeast SEC12 functionally, in contrast with the *Arabidopsis* STL2P protein. Second, the plasma membrane localization of PIP2A is retained in *phf1* mutants, and RNase secretion is also unaltered in *phf1*. Third, SO_4^{2-} uptake, growth under low nitrogen, and responses of *AtIPSI:GUS* to sugar and cytokinins under Pi starvation are not different from those in the wild type. Fourth, the greatest effect of *phf1* mutants revealed by elemental profiling is on Pi content. There are some additional (minor/moderate) differences detected between the wild type and the *phf1* alleles, most of them involving an increase rather than a decrease in the content of ions in the mutant, which could be explained by ionic homeostasis, in agreement with the findings of Lahner et al. (2003). Finally, *PHF1* expression data are also in agreement with a specific role of PHF1 in Pi transport.

PHF1 is responsive to Pi starvation and not to other types of nutrient deficiency, suggesting that its principal role is in P nutrition. Like other Pi starvation–responsive genes, *PHF1* expression is stimulated by sugars and repressed by cytokinins. Additionally, *PHF1* expression is reduced in the *phr1* mutant. The effect of the *phr1* mutation on *PHF1* expression, although only moderate, is similar to the effect of this mutation on the expression of other genes of the Pi starvation rescue system, such as *PHT1;1*, which has been proposed to reflect partial redundancy between PHR1 and closely related homologs present in *Arabidopsis* (Rubio et al., 2001). In fact, both the *Arabidopsis* and rice *PHF1* genes share a conserved motif, GAATATCC, conforming to the PHR1 core binding sequence (GNATATNC; Rubio et al., 2001), within a 300-nucleotide region upstream of the start codon of the encoded protein (P < 0.000001), suggesting that *PHF1* is indeed under direct transcriptional control by PHR1 (and/or closely related homologs). *PHF1* is also expressed at a low level in all plant parts when grown in a Pi-sufficient medium, particularly in roots, flowers, and senescing leaves. In this regard, its expression pattern resembles the sum of the expression patterns of all Pi transporter genes (Mudge et al., 2002) rather than that specific to *PHT1;1*, suggesting that PHF1 action is not restricted to PHT1;1 but also includes other members of the PHT1 family.

The fact that the *phf1* mutations are apparently more affected in Pi uptake than the *pht1;1 pht1;4* double mutant is also in agreement with a role of PHF1 in the ER exit of PHT1 transporters other than PHT1;1. Thus, cellular Pi content in both *phf1* alleles reported here is reduced to ∼25% of the level in wild-type plants when grown under a Pi-rich regimen (Figure 1C), whereas the Pi content of the *pht1;1 pht1;4* double mutant is not reduced to

<60% of the wild-type level when grown in a wide range of Pi concentrations (from 0.1 to 1 mM; see Figure 4 in Shin et al., 2004). Such a difference is difficult to explain exclusively on the basis of the different growth conditions in the plants in which measurements were made.

The significant degree of specificity of PHF1 on PHT1;1 (and probably related Pi transporters) among all of the nutrient transporters and other plasma membrane proteins indicates that PHF1 is an accessory protein facilitating the ER exit of members of the PHT1 family (at least of PHT1;1). Given that we only detected PHF1 in the ER and not in COPII vesicles, we tentatively classify PHF1 as an outfitter, an ER-resident accessory protein (Herrmann et al., 1999), although we cannot exclude the possibility that PHF1 escaped detection in COPII. It is unlikely that, despite overall structural conservation between the proteins and their similar subcellular localizations, PHF1 exerts its role in a way mechanistically similar to SEC12 (i.e., by initiating the formation of COPII vesicles specialized in the trafficking of Pi transporters through interaction with and activation of the SAR1 GTPase). In this regard, PHF1 proteins lack 9 out of 10 of the fully conserved residues in SEC12 proteins, and some of these residues were found to be critical for the SEC12 guanine exchange factor catalytic activity and interaction with SAR1 (Futai et al., 2004). One possibility is that PHF1 assists the maturation of PHT1;1 and related proteins in the ER so that they can assume a conformation competent for trafficking (i.e., PHF1 acts as a packaging chaperone). In agreement with this possibility, a reduction or an increase of PHF1 activity (either via mutation or overexpression) results in a parallel reduction or increase of PHT1;1 accumulation, despite an opposite effect on *PHT1;1* RNA accumulation. Also in agreement with a role of PHF1 as a packaging chaperone, *PHF1* expression has been shown to be induced by treatments triggering the unfolded protein response, as detected in microarray-based expression studies (Martínez and Chrispeels, 2003).

In addition, PHF1 also might affect the entry of PHT1;1 (and presumably related proteins) into transport vesicles by specifically recruiting COPII proteins to the ER region rich in these specific cargoes and then being displaced by the cargo before COPII vesicle budding. Further analyses, such as the study of PHF1 interactions with Pi transporters and with COPII components, should provide more information on the exact mechanism of action of PHF1.

PHF1 displays striking functional resemblance to the yeast protein PHO86. Like PHF1, PHO86 is localized in the ER and impairment of PHO86 function results in the accumulation of the PHT1-related yeast Pi transporter PHO84 in the ER instead of the plasma membrane. Moreover, both PHF1 and PHO86 are responsive to Pi starvation. However, PHF1 and PHO86 are structurally unrelated. No sequence similarity can be detected between these two proteins, and whereas PHO86 has four predicted transmembrane domains, PHF1 has only one. In yeast, known accessory proteins such as GSF2, SHR3, and ERV14, which are involved in the ER exit of specific hexose transporters, specific amino acid permeases, and a membrane glycoprotein, respectively, display strikingly different structures (Gilstring et al., 1999; Sherwood and Carlson, 1999; Powers and Barlowe, 2002). The fact that PHF1 and PHO86 both act on closely related proteins (Pi transporters) strongly suggests that the existence of structural

diversity among accessory proteins reflects fairly loose structural constraints for performing this type of function. In this context, we propose that plants and yeast exploited the limited structural constraints on accessory proteins to evolve accessory proteins for trafficking of their Pi transporters independently and to adjust to their specific (sub)cellular environment, particularly in the endomembrane system.

In summary, we have identified a novel component of the P nutrition system in plants, represented by PHF1, that reveals the existence of ER exit accessory proteins in plants and that they may have evolved independently in the plant phyla. The existence of cargo-specific accessory proteins argues against an exclusive bulk-flow model for the ER exit of proteins entering the secretory pathway in plants. Finally, accessory proteins potentially introduce an additional level of control of the activity of the proteins dependent on them for subcellular localization.

METHODS

Plant Material and Growth Conditions

Arabidopsis thaliana ecotypes used in this study were Col-0 and L*er*. Growth conditions and media were as described previously (Rubio et al., 2001), except where indicated for nutrient, sucrose, and hormone concentrations. In the Pi-lacking medium, KH_2PO_4 was replaced by equimolar amounts of KCl; in nitrogen-lacking medium, $Ca(NO_3)_2$ and KNO_3 were replaced by $CaCl_2$ and K_2SO_4, respectively; in K-lacking medium, KH_2PO_4, KNO_3, KCl, and KOH were replaced by NaH_2PO_4, $NaNO_3$, NaCl, and NaOH respectively; in iron-deficient medium, $FeSO_4$ was removed; and in sulfur-lacking medium, $MgSO_4$, $MnSO_4$, $ZnSO_4$, and $CuSO_4$ were replaced by $Mg(NO_3)_2$, $MnCl_2$, $ZnCl_2$, and $CuCl_2$, respectively. Arsenate resistance was examined in Pi-lacking medium supplemented with $Na_2AsO_4·H_2O$ (10 ppm).

Physiological Measurements

Cellular Pi was measured according to the method of Ames (1966) in plants grown for 12 d in complete or Pi-lacking medium. Pi and SO_4^{2-} uptake experiments were performed as described by Narang et al. (2000) with minor modification. Plants were grown for 8 d in solid complete medium except for Pi or SO_4^{2-}, the concentration of which was reduced to 60 μM. Uptake measurements were made after incubation of submerged roots of plants in a solution with a ^{32}Pi or $^{35}SO_4^{2-}$ concentration corresponding to complete medium. Elemental analysis was performed by the Serveis Cientificotècnics of the Universitat de Barcelona, except the C, N, and S analyses, which were performed by the Elemental Microanalysis Center at the Universidad Complutense de Madrid. Whole plant samples were dried for 48 h and subsequently digested with HNO_3 and H_2O_2 at 200°C and with HF at 120°C. Ca, Na, K, P, Fe, and Zn were determined by inductively coupled plasma emission spectroscopy using the Perkin-Elmer Optima 3200 RL equipment. Mn, Cu, Mo, and Cd were performed by inductively coupled plasma–mass spectrometry using Perkin-Elmer ELAN 6000 equipment. C, N, and S were determined by combustion at 1200°C of powdered plants using a LECO CHNS 932 analyzer. Mean values were compared by use of Student's *t* test.

Genetic Analysis and Positional Cloning of *phf1*

phf1 mutant plants were backcrossed three times to wild-type plants (Col-0) to test the linkage of the different phenotypes to a single recessive mutation. For mapping purposes, *phf1-1* plants (Col-0 ecotype) were crossed to wild-type plants of the L*er* ecotype. DNA from F2 seedlings displaying mutant phenotypes was prepared and used to analyze the linkage of the *phf1-1* mutation to previously described simple sequence length polymorphism (Bell and Ecker, 1994) and cleaved-amplified polymorphic sequence (Konieczny and Ausubel, 1993) markers. PHF1 was mapped to chromosome 3 between ALS1 and AFC1 markers. To identify the mutant gene, the Cereon collection of nucleotide polymorphisms between ecotypes Col and L*er* (http://www.arabidopsis.org/cereon/index.html) was used to generate new markers in the area surrounding *PHF1*.

Molecular Procedures

Routine molecular work was performed as described previously, except where indicated (Sambrook et al., 1989; Rubio et al., 2001). The sequences of the PCR primers used for amplification of different genomic DNA/cDNA fragments are given in Supplemental Table 1 online.

Constructs for Expression in Plants and Plant Transformation

For complementation experiments, a 6-kb genomic fragment of DNA containing the coding region of *PHF1* was amplified by PCR. The PCR product was cloned into pBIB (Becker, 1990), generating *gPHF1*. The *PHF1* cDNA was obtained by RT-PCR and cloned into pBIB35S, a 35S promoter–containing vector derived from pBIB.

Fusions to GFP were made using the pGWB vectors based on Clontech Gateway technology (kindly provided by Tsuyoshi Nakagawa). The genomic fragments for the *PHF1:GFP* and *PHT1;1:GFP* constructs were cloned into pGWB4. The genomic fragments (coding region) for the *35S:PHF1:GFP* and *35S:PHT1;1:GFP* constructs were cloned into pGWB5. In all cases, the resulting vectors were introduced into the C58CI strain of *Agrobacterium tumefaciens*, and *Arabidopsis phf1* plants were transformed as described (Bechtold et al., 1993).

The ER marker gene (*35S:DsRed2:KDEL*) was constructed according to Haseloff et al. (1997) and cloned into the pAVA393 vector (Siemering et al., 1996) by changing *GFP5* for *DsRed2*. The *35S:DsRed2:KDEL* fusion was transiently expressed by particle bombardment into leaves of *Arabidopsis* plants harboring the *35S:PHF1:GFP* construct, using a helium-driven particle accelerator (PDS-1000/He; Bio-Rad) according to the manufacturer's recommendations. Five micrograms of plasmid was used for each transformation event. Leaves were transferred for 48 h to Pi-lacking medium before microscopic analysis.

Yeast Transformation and Constructs

Complementation tests in yeasts were performed using *PHF1* and *STL2P* open reading frames (d'Enfert et al., 1992) cloned into p181A1NE (Leggewie et al., 1997). Transformation of the resulting constructs into the *Saccharomyces cerevisiae sec12* mutant (RSY653; d'Enfert et al., 1991) was made according to Gietz and Woods (2002). Transformants were grown on yeast peptone dextrose medium at 25 and 37°C for 3 d.

Fluorescence Microscopy

Bombarded tissues and transgenic plants were first screened at low magnification using an epifluorescence microscope (Leica DM-R). GFP fluorescence was excited at 470/40 nm and subsequently passed through a 525/50-nm emission filter. DsRed2 was excited at 546/10 nm and subsequently passed through a 590-nm emission filter. Plant tissues were dissected and mounted in water for viewing with a Zeiss Axiovert 200 confocal microscope coupled to the Bio-Rad Radiance 2100 laser scanning confocal imaging system with LaserSharp version 5 imaging software. GFP fluorescence was excited at 488 nm using an argon ion laser and subsequently passed through a 515/30-nm emission filter excluding chlorophyll autofluorescence. DsRed2 was excited at 543 nm using a helium/neon laser and subsequently passed through a 570LP emission filter. Before preliminary screening and confocal microscopy, the seedlings were stained with propidium iodide (Mudge et al., 2002) to

avoid cell wall autofluorescence produced by excitation at 470/40 nm and 488 nm.

Biochemical Analysis of Proteins

To assay for secreted RNase activity, plants were grown in complete liquid medium for 5 d and then transferred to Pi-sufficient or Pi-deficient medium for 7 d. The liquid medium was collected for analysis. Protein (25 μg/sample) was loaded onto 12% Tris-Gly nondenaturing PAGE gels (NuPAGE system; Invitrogen). Staining for RNase activity on native gels was performed as described by Abel and Glund (1986).

The analysis of PHT1;1:GFP by protein gel blotting was as follows. Plantlets were ground to powder in liquid nitrogen and extracted in Laemmli buffer (Laemmli, 1970). Protein (25 μg/sample) was loaded onto 4 to 12% Bis-Tris SDS-PAGE gels (NuPAGE system) and then transferred to nylon membranes (Amersham). PHT1;1:GFP was detected with anti-GFP antibodies (Roche Diagnostics), and bands were revealed by Supersignal West Pico chemiluminescent substrate (Pierce). Finally, membranes were stained with Coomassie Brilliant Blue R 250 (Sambrook et al., 1989).

Protein Structure Prediction and Phylogenetic Analysis

Databank searches (Swissprot, European Molecular Biology Laboratory, and National Center for Biotechnology Information) were performed using the BLAST program (Altschul et al., 1990). Sequence alignment was made using the T-COFFEE program (Notredame et al., 2000; http://www.ch.embnet.org/software/TCoffee.html). Structural prediction was made using GENESILICO (Kurowski and Bujnicki, 2003; http://genesilico.pl/meta) and the SMART program (Letunic et al., 2004). The phylogram was constructed based on the alignment obtained with T-COFFEE and the PROTPARS program of the PHYLIP software package (Felsenstein, 1989; http://evolution.genetics.washington.edu/phylip/doc/main.html). Samples for bootstrapping (1000 samples) and the consensus tree and bootstrapping values were obtained with the SEQBOOT and CONSENSE programs, respectively, also from the PHYLIP software package. Visualization of the tree was performed using the ATV program (http://www.genetics.wustl.edu/eddy/atv/).

Accession Numbers

Sequence data from this article can be found in the Arabidopsis Genome Initiative/GenBank data libraries under the following accession numbers: *PHF1* (*Arabidopsis* PHF1), At3g52190; LePHF1 (*Lycopersicon esculentum* PHF1), 47105805; OsPHF1 (*Oryza sativa* PHF1), 32984969; *STL2P* (*Arabidopsis* SEC12 ortholog), At2g01470; OsSEC12 (*O. sativa* SEC12 ortholog), 37988440; CeSEC12 (*Caenorhabditis elegans* SEC12 ortholog), 17508005; DmSEC12 (*Drosophila melanogaster* SEC12 ortholog), 7297075; HsPREB (*Homo sapiens* SEC12 ortholog), 17368974; ScSEC12 (*Saccharomyces cerevisiae* SEC12), 6325353; SpSTL1 (*Schizosaccharomyces pombe* SEC12 ortholog), 173493.

Supplemental Data

The following materials are available in the online version of this article.

Supplemental Table 1. Oligonucleotides Used for the Preparation of the Different Constructs.

Supplemental Figure 1. Alignment of *Arabidopsis* PHF1 with Presumed Functional PHF1 Homologs and with SEC12 Proteins Using the Program T-COFFEE.

Supplemental Figure 2. Complementation of *phf1* with Constructs Expressing a Functional PHF1:GFP Fusion Protein.

Supplemental Figure 3. Subcellular Localization of PHT1;1:GFP in Wild-Type Plants Grown under a Pi-Rich Regimen.

REFERENCES

Abel, S., and Glund, K. (1986). Localisation of RNA-degrading enzyme activity within vacuoles of cultured tomato cells. Physiol. Plant. **66,** 79–86.

Altschul, S.F., Gish, W., Miller, W., Myers, E.W., and Lipman, D.J. (1990). Basic local alignment search tool. J. Mol. Biol. **215,** 403–410.

Ames, B.N. (1966). Assay of inorganic phosphate, total phosphate and phosphatases. Methods Enzymol. **8,** 115–118.

Asher, C.J., and Reay, P.F. (1979). Arsenic uptake by barley seedlings. Aust. J. Plant Physiol. **6,** 459–466.

Barlowe, C. (2003). Signals for COPII-dependent export from the ER: What's the ticket out? Trends Cell Biol. **13,** 295–300.

Barlowe, C., and Schekman, R. (1993). SEC12 encodes a guanine-nucleotide-exchange factor essential for transport vesicle budding from the ER. Nature **365,** 347–349.

Bechtold, N., Ellis, J., and Pelletier, G. (1993). In planta *Agrobacterium* mediated gene transfer by infiltration of adult *Arabidopsis thaliana* plants. C. R. Acad. Sci. Paris Life Sci. **316,** 15–18.

Becker, D. (1990). Binary vectors which allow the exchange of plant selectable markers and reporter genes. Nucleic Acids Res. **18,** 203.

Bell, C.J., and Ecker, J.R. (1994). Assignment of 30 microsatellite loci to the linkage map of *Arabidopsis.* Genomics **19,** 137–144.

Chardin, P., and Callebaut, I. (2002). The yeast Sar exchange factor Sec12, and its higher organism orthologs, fold as beta-propellers. FEBS Lett. **525,** 171–173.

Chiou, T.J., Liu, H., and Harrison, M.J. (2001). The spatial expression patterns of a phosphate transporter (MtPT1) from *Medicago truncatula* indicate a role in phosphate transport at the root/soil interface. Plant J. **25,** 281–293.

Crofts, A.J., Leborgne-Castel, N., Hillmer, S., Robinson, D.G., Phillipson, B., Carlsson, L.E., Ashford, D.A., and Denecke, J. (1999). Saturation of the endoplasmic reticulum retention machinery reveals anterograde bulk flow. Plant Cell **11,** 2233–2248.

Cutler, S.R., Ehrhardt, D.W., Griffitts, J.S., and Somerville, C.R. (2000). Random GFP:cDNA fusions enable visualisation of subcellular structures in cells of *Arabidopsis* at a high frequency. Proc. Natl. Acad. Sci. USA **97,** 3718–3723.

d'Enfert, C., Barlowe, C., Nishikawa, S., Nakano, A., and Schekman, R. (1991). Structural and functional dissection of a membrane glycoprotein required for vesicle budding from the endoplasmic reticulum. Mol. Cell. Biol. **11,** 5727–5734.

d'Enfert, C., Gensse, M., and Gaillardin, C. (1992). Fission yeast and a plant have functional homologues of the Sar1 and Sec12 proteins

involved in ER to Golgi traffic in budding yeast. EMBO J. **11,** 4205–4211.

Dunkley, T.P., Watson, R., Griffin, J.L., Dupree, P., and Lilley, K.S. (2004). Localisation of organelle proteins by isotope tagging (LOPIT). Mol. Cell. Proteomics **3,** 1128–1134.

Felsenstein, J. (1989). PHYLIP—Phylogeny Inference Package (version 3.2). Cladistics **5,** 164–166.

Franco-Zorrilla, J.M., Gonzalez, E., Bustos, R., Linhares, F., Leyva, A., and Paz-Ares, J. (2004). The transcriptional control of plant responses to phosphate limitation. J. Exp. Bot. **55,** 285–293.

Franco-Zorrilla, J.M., Martin, A.C., Leyva, A., and Paz-Ares, J. (2005). Interaction between phosphate-starvation, sugar and cytokinin signalling in *Arabidopsis* and the roles of cytokinin receptors CRE1/AHK4 and AHK3. Plant Physiol. **138,** 847–857.

Futai, E., Hamamoto, S., Orci, L., and Schekman, R. (2004). GTP/GDP exchange by Sec12p enables COPII vesicle bud formation on synthetic liposomes. EMBO J. **23,** 4146–4155.

Gietz, R.D., and Woods, R.A. (2002). Transformation of yeast by the LiAc/SS carrier DNA/PEG method. Methods Enzymol. **350,** 87–96.

Gilstring, C.F., Melin-Larsson, M., and Ljungdahl, P.O. (1999). Shr3p mediates specific COPII coatomer-cargo interactions required for the packaging of amino acid permeases into ER-derived transport vesicles. Mol. Biol. Cell **10,** 3549–3565.

Goff, S.A., et al . (2002). A draft sequence of the rice genome (*Oryza sativa* L. ssp. *japonica*). Science **296,** 92–100.

Haseloff, J., Siemering, K.R., Prasher, D.C., and Hodge, S. (1997). Removal of a cryptic intron and subcellular localisation of green fluorescent protein are required to mark transgenic *Arabidopsis* plants brightly. Proc. Natl. Acad. Sci. USA **94,** 2122–2127.

Herrmann, J.M., Malkus, P., and Schekman, R. (1999). Out of the ER—Outfitters, escorts and guides. Trends Cell Biol. **9,** 5–7.

Jurgens, G. (2004). Membrane trafficking in plants. Annu. Rev. Cell Dev. Biol. **20,** 481–504.

Karthikeyan, A.S., Varadarajan, D.K., Mukatira, U.T., D'Urzo, M.P., Damsz, B., and Raghothama, K.G. (2002). Regulated expression of *Arabidopsis* phosphate transporters. Plant Physiol. **130,** 221–233.

Konieczny, A., and Ausubel, F.M. (1993). A procedure for mapping *Arabidopsis* mutations using co-dominant ecotype-specific PCR-based markers. Plant J. **4,** 403–410.

Kurowski, M.A., and Bujnicki, J.M. (2003). GENESILICO protein structure prediction meta-server. Nucleic Acids Res. **31,** 3305–3307.

Laemmli, U.K. (1970). Cleavage of structural proteins during the assembly of the head of bacteriophage T4. Nature **227,** 680–685.

Lahner, B., Gong, J., Mahmoudian, M., Smith, E.L., Abid, K.B., Rogers, E.E., Guerinot, M.L., Harper, J.F., Ward, J.M., McIntyre, L., Schroeder, J.I., and Salt, D.E. (2003). Genomic scale profiling of nutrient and trace elements in *Arabidopsis thaliana*. Nat. Biotechnol. **21,** 1215–1221.

Lau, W.T., Howson, R.W., Malkus, P., Schekman, R., and O'Shea, E.K. (2000). Pho86p, an endoplasmic reticulum (ER) resident protein in *Saccharomyces cerevisiae*, is required for ER exit of the high-affinity phosphate transporter Pho84p. Proc. Natl. Acad. Sci. USA **97,** 1107–1112.

Leggewie, G., Willmitzer, L., and Riesmeier, J.W. (1997). Two cDNAs from potato are able to complement a phosphate uptake-deficient yeast mutant: Identification of phosphate transporters from higher plants. Plant Cell **9,** 381–392.

Lejay, L., Gansel, X., Cerezo, M., Tillard, P., Muller, C., Krapp, A., von Wiren, N., Daniel-Vedele, F., and Gojon, A. (2003). Regulation of root ion transporters by photosynthesis: Functional importance and relation with hexokinase. Plant Cell **15,** 2218–2232.

Letunic, I., Copley, R.R., Schmidt, S., Ciccarelli, F.D., Doerks, T.,

Schultz, J., Ponting, C.P., and Bork, P. (2004). SMART 4.0: Towards genomic data integration. Nucleic Acids Res. **32,** D142–D144.

Martin, A.C., del Pozo, J.C., Iglesias, J., Rubio, V., Solano, R., de La Peña, A., Leyva, A., and Paz-Ares, J. (2000). Influence of cytokinins on the expression of phosphate starvation responsive genes in *Arabidopsis.* Plant J. **24,** 559–567.

Martínez, I.M., and Chrispeels, M.J. (2003). Genomic analysis of the unfolded protein response in *Arabidopsis* shows its connection to important cellular processes. Plant Cell **15,** 561–576.

Misson, J., et al . (2005). A genome-wide transcriptional analysis using *Arabidopsis thaliana* Affymetrix gene chips determined plant responses to phosphate deprivation. Proc. Natl. Acad. Sci. USA **102,** 11934–11939.

Mudge, S.R., Rae, A.L., Diatloff, E., and Smith, F.W. (2002). Expression analysis suggests novel roles for members of the Pht1 family of phosphate transporters in *Arabidopsis.* Plant J. **31,** 341–353.

Narang, R.A., Bruene, A., and Altmann, T. (2000). Analysis of phosphate acquisition efficiency in different *Arabidopsis* accessions. Plant Physiol. **124,** 1786–1799.

Neumann, U., Brandizzi, F., and Hawes, C. (2003). Protein transport in plant cells: In and out of the Golgi. Ann. Bot. (Lond.) **92,** 167–180.

Notredame, C., Higgins, D.G., and Heringa, J. (2000). T-Coffee: A novel method for fast and accurate multiple sequence alignment. J. Mol. Biol. **302,** 205–217.

Phillipson, B.A., Pimpl, P., daSilva, L.L., Crofts, A.J., Taylor, J.P., Movafeghi, A., Robinson, D.G., and Denecke, J. (2001). Secretory bulk flow of soluble proteins is efficient and COPII dependent. Plant Cell **13,** 2005–2020.

Powers, J., and Barlowe, C. (2002). Erv14p directs a transmembrane secretory protein into COPII-coated transport vesicles. Mol. Biol. Cell **13,** 880–891.

Raghothama, K.G. (1999). Phosphate acquisition. Annu. Rev. Plant Physiol. Plant Mol. Biol. **50,** 665–693.

Rausch, C., and Bucher, M. (2002). Molecular mechanisms of phosphate transport in plants. Planta **216,** 23–37.

Rubio, V., Linhares, F., Solano, R., Martin, A.C., Iglesias, J., Leyva, A., and Paz-Ares, J. (2001). A conserved MYB transcription factor involved in phosphate starvation signalling both in vascular plants and in unicellular algae. Genes Dev. **15,** 2122–2133.

Sambrook, J., Fritsch, E.F., and Maniatis, T. (1989). Molecular Cloning: A Laboratory Manual, 2nd ed. (Cold Spring Harbor, NY: Cold Spring Harbor Laboratory Press).

Sanderfoot, A.A., and Raikhel, N.V. (2003). The secretory system of *Arabidopsis.* In The Arabidopsis Book, C.R. Somerville and E.M. Meyerowitz, eds (Rockville, MD: American Society of Plant Biologists), doi 10.1199/tab.0098, http://www.aspb.org/publications/ arabidopsis/.

Sherwood, P.W., and Carlson, M. (1999). Efficient export of the glucose transporter Hxt1p from the endoplasmic reticulum requires Gsf2p. Proc. Natl. Acad. Sci. USA **96,** 7415–7420.

Shin, H., Shin, H.S., Dewbre, G.R., and Harrison, M.J. (2004). Phosphate transport in *Arabidopsis*: Pht1;1 and Pht1;4 play a major role in phosphate acquisition from both low- and high-phosphate environments. Plant J. **39,** 629–642.

Siemering, K.R., Golbik, R., Sever, R., and Haseloff, J. (1996). Mutations that suppress the thermosensitivity of green fluorescent protein. Curr. Biol. **6,** 1653–1663.

Sprague, E.R., Redd, M.J., Johnson, A.D., and Wolberger, C. (2000). Structure of the C-terminal domain of Tup1, a corepressor of transcription in yeast. EMBO J. **19,** 3016–3027.

Ticconi, C.A., and Abel, S. (2004). Short on phosphate: Plant surveillance and countermeasures. Trends Plant Sci. **9,** 548–555.